

Description of nuclear octupole and quadrupole deformation close to the axial symmetry: Octupole vibrations in the X(5) nuclei ^{150}Nd and ^{152}Sm

P.G. Bizzeti* and A.M. Bizzeti-Sona
 Dipartimento di Fisica, Università di Firenze
 I.N.F.N., Sezione di Firenze
 Via G. Sansone 1, 50019 Sesto Fiorentino (Firenze), Italy
 (Dated: January 4, 2019)

The model, introduced in a previous paper, for the description of the octupole and quadrupole degrees of freedom in conditions close to the axial symmetry, is used to describe the negative-parity band based on the first octupole vibrational state in nuclei close to the critical point of the U(5) to SU(3) phase transition. The situation of ^{150}Nd and ^{152}Sm is discussed in detail. The positive parity levels of these nuclei, and also the in-band E2 transitions, are reasonably accounted for by the X(5) model. With simple assumptions on the nature of the octupole vibrations, it is possible to describe, with comparable accuracy, also the negative parity sector, without changing the description of the positive-parity part.

PACS numbers: 21.60.Ev

I. INTRODUCTION

In a previous paper [1] (henceforth referred to as I) a simple model has been introduced to describe the phase transitions in nuclear shape involving the octupole mode. This model, valid for nuclear shapes close to the axial symmetry, has been used to describe transitional nuclei in the Radium – Thorium region. The phase transition between octupole vibration and axial octupole deformation, in nuclei which already possess a stable (axial) quadrupole deformation has been investigated, and the model has been found to account for the properties of Thorium isotopes $^{226,228}\text{Th}$. In a second paper [2] the analysis has been extended to the case of phase transitions involving at the same time the axial quadrupole and octupole degrees of freedom (from harmonic vibrations around a spherical shape to a permanent, reflection asymmetric, axial deformation). In particular, the X(5)-like nuclei ^{224}Ra and ^{224}Th were found to correspond well to this situation, and their $K = 0$ bands agree well with the model predictions, as well in the negative parity sector as in the positive parity one [2].

In the present part of our work, we are going to consider the effect of axial octupole vibrations of small amplitude, around a reflection symmetric shape, in nuclei at the critical point between spherical shape and axial quadrupole deformation, corresponding to the quasi-symmetry X(5) [3]. This is apparently the case for the two early examples of critical-point nuclei, ^{152}Sm [4] and ^{150}Nd [5]. In these two nuclides, the positive parity sector of the level scheme is well described by the X(5) model, while a 1^- state with excitation energy significantly larger than that of the lowest 2^+ state (see Figs. 1,2) can be interpreted as the lowest state of octupole excitation. A $\Delta J = 2$ band is built over this

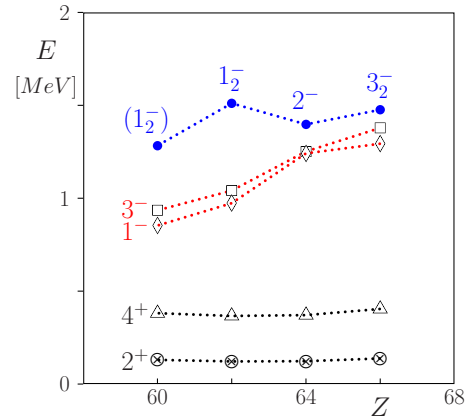


FIG. 1: (color on line) Excitation energies of the lowest levels 1^- , 2^+ , 3^- and 4^+ in the $N = 90$ isotones $^{150}_{60}\text{Nd}$, $^{152}_{62}\text{Sm}$, $^{154}_{64}\text{Gd}$ and $^{156}_{66}\text{Dy}$. The lowest negative-parity levels not belonging to the $K^\pi = 0^-$ sequence are shown as full dots.

1^- state, and the absence of even- J states shows that a quantum number $K = 0$ can be attributed to it, indicating an axially symmetric character for the octupole excitation. As $K \neq 0$ bands do not appear at similar excitation energy, this situation should be suitable to be described by the model introduced in I.

Actually, nuclear systematics [6] and several self-consistent calculations (see, *e.g.*, [7–9]) indicate that such a shape phase transition can take place in a wider region around ^{152}Sm . In fact, level schemes very close to that of the X(5) model are found also in the heavier $N = 90$ nuclei ^{154}Gd and ^{156}Dy (but only in ^{154}Gd the relative $B(E2)$ values follow the X(5) predictions) [10, 11]. However, in these nuclei the excitation energy of the lowest 1^- level increases, and approaches that of the lowest negative-parity level not belonging to the $K^\pi = 0^-$ sequence (Fig. 1): therefore, they cannot be treated in the frame of our model, which is intended for nuclear shapes having an approximate (not necessarily exact) axial sym-

*Electronic address: bizzeti@fi.infn.it

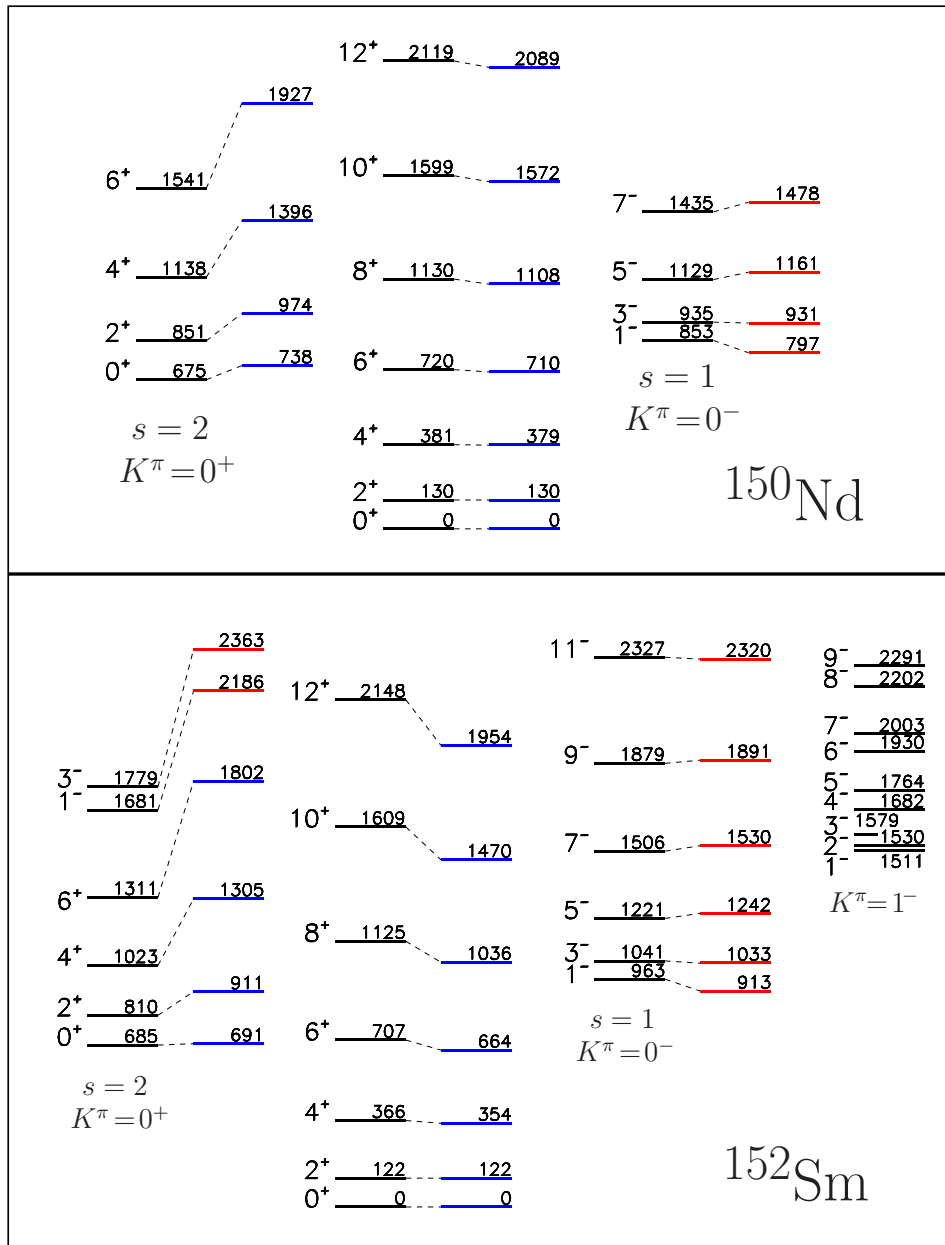


FIG. 2: (color on line) Partial level schemes of ^{150}Nd and ^{152}Sm . For each band, the experimental values (left) are compared with the model predictions (right) with constant $\Delta_k:\Delta_0 = 0$ (X(5) model) for even J and parity, $\Delta_1 = 15$ or $\Delta_1 = 20$ for states with odd J and parity of ^{150}Nd or ^{152}Sm , respectively (see Section III). Theoretical values of the excitation energies (in keV) are normalized to that of the 2_1^+ level. Negative-parity levels belonging to the $s = 2$ sequence of ^{152}Sm are shown in the same column as the positive-parity ones. Higher lying negative parity states of ^{152}Sm , apparently belonging to a $K^\pi = 1^-$ band, are also shown at the right-hand margin.

metry [1].

As already noted in [12], in the critical-point nuclei ^{150}Nd and ^{152}Sm the level spacings in the $K^\pi = 0^-$ band do not follow the same pattern of those of the ground-state band, as it is (approximately) the case for the bands based on one or two phonons of γ vibration. Therefore, the lowest negative parity band cannot be explained assuming an approximate decoupling of axial octupole and

quadrupole modes, based on the same intrinsic configuration. Instead, we can assume that also in the present case, as in the case of light Thorium isotopes [1, 2], an intimate connection exists between the axial quadrupole and octupole modes, in spite of the fact that the latter is characterized by a much larger excitation energy. As we shall see, a simple model based on this assumption is able to reproduce the negative parity band with an accu-

racy comparable to that attained by the X(5) model in explaining the positive parity states.

For convenience of the reader, the main results of our model are summarized in the next Section II. In Sections III and IV, the model is specialized to the present case. Finally, in Section V, empirical data concerning ^{152}Sm and ^{150}Nd are discussed on the basis of this theoretical model.

Preliminary results of this work have been presented at the XIV International Workshop on Nuclear Theory (Rila, Bulgaria, 2005) [13] and in the 2006 Predeal Summer School in Nuclear Physics [14].

II. THE BASES OF THE MODEL

Our model is an extension of Bohr's hydrodynamic model [15], to include also axial octupole deformations. Non-axial deformations (of quadrupole or octupole character) are only considered up to the first order in the corresponding parameters, as well as the variables describing the possible misalignment of the tensors of inertia corresponding to octupole deformation or to quadrupole deformation alone.

Following the conventions introduced in I, we choose as the intrinsic reference frame the one referred to the principal axes of the overall tensor of inertia, resulting from the combined effects of quadrupole and octupole deformation. Moreover, our dynamical variables $a_\mu^{(\lambda)}$ ($\lambda = 2, 3$; $\mu = -\lambda \dots \lambda$), describing the nuclear deformations of different orders, are considered to include the corresponding inertial parameter, so that our variable $a_\mu^{(\lambda)}$ corresponds to $\sqrt{B_\lambda} a_\mu^{(\lambda)}$ in the original notations of Bohr. The set of deformation variables $a_\mu^{(\lambda)}$ is parametrized in terms of new dynamical variables,

$$\begin{aligned}
a_0^{(2)} &= \beta_2 \cos \gamma_2 \approx \beta_2 & (1) \\
a_1^{(2)} &= -\frac{\sqrt{2} \beta_3}{\sqrt{\beta_2^2 + 2\beta_3^2}} v (\sin \varphi + i \cos \varphi) \\
a_2^{(2)} &= \sqrt{1/2} \beta_2 \sin \gamma_2 - i \frac{\sqrt{5} \beta_3}{\sqrt{\beta_2^2 + 2\beta_3^2}} u \sin \chi \\
a_0^{(3)} &= \beta_3 \cos \gamma_3 \approx \beta_3 \\
a_1^{(3)} &= \frac{\sqrt{5} \beta_2}{\sqrt{\beta_2^2 + 2\beta_3^2}} v (\sin \varphi + i \cos \varphi) \\
a_2^{(3)} &= \sqrt{1/2} \beta_3 \sin \gamma_3 + i \frac{\beta_2}{\sqrt{\beta_2^2 + 2\beta_3^2}} u \sin \chi \\
a_3^{(3)} &= w \sin \vartheta \left[\cos \gamma_3 + (\sqrt{15}/2) \sin \gamma_3 \right] \\
&\quad + i w \cos \vartheta \left[\cos \gamma_3 - (\sqrt{15}/2) \sin \gamma_3 \right] \\
&\approx w (\sin \vartheta + i \cos \vartheta)
\end{aligned}$$

In the above expressions, non-axial degrees of freedom are taken into account only up to the first order in the

corresponding amplitudes¹. Finally, the variables γ_2 and γ_3 are expressed as

$$\begin{aligned}
\gamma_2 &= \frac{\sqrt{10} \beta_3}{\beta_2 \sqrt{\beta_2^2 + 5\beta_3^2}} u \cos \chi + \frac{f(\beta_2, \beta_3)}{\sqrt{\beta_2^2 + 5\beta_3^2}} u_0 & (2) \\
\gamma_3 &= -\frac{\sqrt{2} \beta_2}{\beta_3 \sqrt{\beta_2^2 + 5\beta_3^2}} u \cos \chi + \frac{\sqrt{5} f(\beta_2, \beta_3)}{\sqrt{\beta_2^2 + 5\beta_3^2}} u_0
\end{aligned}$$

With this choice, the tensor of inertia turns out to be diagonal *up to the first order in the small variables* $u_0, u, v, w, \vartheta, \varphi$, and χ . Up to this point, the form of the function $f(\beta_2, \beta_3)$ is left completely free. In [2] a possible choice for this function is introduced, namely $f(\beta_2, \beta_3) = \sqrt{(\beta_2^2 + \beta_3^2)(\beta_2^2 + 2\beta_3^2)/(\beta_2^2 + 5\beta_3^2)}$, to obtain the proper basis for the description of a critical point in both the (axial) quadrupole and octupole degrees of freedom. With this choice, the determinant of the matrix of inertia takes the form

$$G \propto \frac{(\beta_2^2 + \beta_3^2)^2 (\beta_2^2 + 2\beta_3^2)^4}{(\beta_2^2 + 5\beta_3^2)^2} u_0^2 v^2 u^2 w^2 \quad (3)$$

and the differential equation in the variables β_2, β_3 that is obtained with the Pauli procedure [19] of quantization (assuming an approximate decoupling from the part involving all other dynamical variables) reduces to the Bohr equation at the limit $\beta_3 \rightarrow 0$. One obtains

$$\begin{aligned}
\frac{1}{g} \left\{ \frac{\partial}{\partial \beta_2} \left[g \frac{\partial \Psi}{\partial \beta_2} \right] + \frac{\partial}{\partial \beta_3} \left[g \frac{\partial \Psi}{\partial \beta_3} \right] \right\} & (4) \\
+ \left\{ \epsilon - V + \frac{A_J}{\beta_2^2 + 2\beta_3^2} \right\} \Psi(\beta_2, \beta_3) &= 0
\end{aligned}$$

where $g \propto G^{1/2}$, $V = V(\beta_2, \beta_3)$ and $A_J = J(J+1)/3$. Due to the time reversal invariance, the potential must be even with respect to β_3 , $V(\beta_2, -\beta_3) = V(\beta_2, \beta_3)$, while the wavefunction Ψ must be even in β_3 for the states of even parity and J and odd for states of odd parity and J .

It is convenient to eliminate from Eq. 4 the first derivative terms, with the substitution

$$\Psi = \Psi_0 / g^{1/2}. \quad (5)$$

The differential equation for $\Psi_0(\beta_2, \beta_3)$ is

$$\begin{aligned}
\frac{\partial^2 \Psi_0}{\partial \beta_2^2} + \frac{\partial^2 \Psi_0}{\partial \beta_3^2} & (6) \\
+ \left\{ \epsilon - V + V_g - \frac{A_J}{\beta_2^2 + 2\beta_3^2} \right\} \Psi_0(\beta_2, \beta_3) &= 0
\end{aligned}$$

¹ The simultaneous treatment of axial and non-axial octupole modes is considered, *e.g.*, in [16, 17] and in [18].

with

$$V_g = \frac{1}{4g^2} \left[\left(\frac{\partial g}{\partial \beta_2} \right)^2 + \left(\frac{\partial g}{\partial \beta_3} \right)^2 \right] - \frac{1}{2g} \left[\frac{\partial^2 g}{\partial \beta_2^2} + \frac{\partial^2 g}{\partial \beta_3^2} \right] \\ = - \frac{2(\beta_2^6 + 37\beta_2^4\beta_3^2 + 107\beta_2^2\beta_3^4 + 95\beta_3^6)}{(\beta_2^2 + 5\beta_3^2)^2(\beta_2^4 + 3\beta_2^2\beta_3^2 + 2\beta_3^4)} \quad (7)$$

In the situation considered in [2], a flat potential extends in a rather wide region in both directions of β_2 and β_3 . The two-dimensional Schroedinger equation cannot be solved analytically, but rather accurate solutions can be obtained by numerical evaluation. We refer to [2] for more details and for the comparison with experimental data.

In the present case, we want to consider, instead, the case where the octupole deformation parameter β_3 is constrained to remain always a small *fraction* of the quadrupole deformation β_2 . As we shall see, introducing a few simplifying assumptions, we obtain results that can be expressed in a close form, as in the case of the standard X(5) model.

III. DETAILS OF THE MODEL AND RESULTS

There is a deep qualitative difference between the structure of the $K = 0$, alternate parity bands of ^{152}Sm , ^{150}Nd and those of the transitional Ra and Th isotopes (see Figs.7 and 9 of [2]). In the latter, the lowest 1^- level lies between the 2^+ and the 4^+ states, and starting from the 5^- the positive- and negative-parity levels follow each other in the increasing order of J . Instead, in ^{152}Sm and ^{150}Nd (Fig. 2), the negative parity levels of angular momentum J are higher than the positive-parity ones of angular momentum $J + 1$ at least up to $J = 14$, and the first 1^- is found between the lowest 6^+ and 8^+ . As the mean square of the deformation parameter for a particular mode of collective excitation is inversely proportional to the energy of the first excitation of this mode, we can conclude that, in the present cases, the octupole deformation is much smaller than the quadrupole one. We will assume that β_3 remains confined to a rather small *fraction* of the quadrupole amplitude β_2 also at the largest values of J . As in [13, 20], we express both (axial) deformation amplitudes in terms of two new variables, β and δ , which will be considered as the independent variables in the following discussion:

$$\beta_2 = \beta \cos \delta \quad (8) \\ \beta_3 = \beta \sin \delta$$

Now, the Eq. 6 can be easily rewritten in terms of the new variables to obtain

$$\frac{\partial^2 \Psi_0}{\partial \beta^2} + \frac{1}{\beta} \frac{\partial \Psi_0}{\partial \beta} + \frac{1}{\beta^2} \frac{\partial^2 \Psi_0}{\partial \delta^2} \\ + \left\{ \epsilon - V + V_g - \frac{A_J}{\beta^2(1 + \sin^2 \delta)} \right\} \Psi_0(\beta, \delta) = 0 \quad (9)$$

where

$$V_g(\beta, \delta) = \frac{1}{\beta^2} [-2 + U_g(\delta)] \quad (10) \\ U_g(\delta) = - \frac{\sin^2 \delta}{1 + \sin^2 \delta} \frac{50 + 24 \sin^2 \delta + 16 \sin^4 \delta}{(1 + 4 \sin^2 \delta)^2}$$

The Eq. 9 results to be separable if the potential $V(\beta, \delta)$ takes the form

$$V(\beta, \delta) = V_\beta(\beta) + \frac{1}{\beta^2} U_\delta(\delta) \quad (11)$$

We can observe that the factor $1/\beta^2$ in the δ -dependent part of the potential becomes irrelevant if $U_\delta(\delta)$ is zero in the interval $-\delta_0 < \delta < \delta_0$ and $+\infty$ outside this interval (as for a typical critical-point potential). With the above choice for the potential, one can put $\Psi_0 = \beta^{-1/2} \psi(\beta) \phi(\delta)$ to obtain the independent differential equations

$$\frac{d^2 \phi_k(\delta)}{d\delta^2} + \left[A'_k(J) - \tilde{U}_\delta(\delta) + \frac{A_J \sin^2 \delta}{1 + \sin^2 \delta} \right] \phi_k(\delta) = 0 \quad (12) \\ \frac{d^2 \psi_k(\beta)}{d\beta^2} + \left[\epsilon_k - \tilde{V}_\beta(\beta) - \frac{A_J + 2 + \Delta_k(J)}{\beta^2} \right] \psi_k(\beta) = 0$$

where $\tilde{U}_\delta = U_\delta - U_g$, while $\Delta_k(J) = A'_k(J) - A'_0(0)$ and $\tilde{V}_\beta(\beta) = V_\beta(\beta) + [A'_0(0) - 1/4]/\beta^2$. The index $k = 0$ corresponds to even parity and J , $k = 1$ to odd parity and J .

The equation in δ contains a weak dependence on J in the term A_J . We shall see that the resulting dependence on J of the separation constant A'_k is actually negligible, at least for not too large values of J . If we neglect it, $\Delta_0 = 0$ and $\Delta_1 \equiv A'_1 - A'_0$ is a constant. We will consider it as an adjustable parameter. We can expect that this approximation remains valid also for different choices of the potential for δ , as long as Eq. 9 remains at least approximately separable.

We must now do some assumptions on the β dependent part of the potential. We know that the positive-parity part of the level scheme is in good agreement with the X(5) predictions. Therefore, the potential term \tilde{V}_β (*not the potential V_β !*) will be taken constant in the interval $0 < \beta \leq \beta_w$ and $= +\infty$ outside, as in the X(5) approximation.

This choice for the potential deserves some more comments. Actually \tilde{V}_β contains, in addition to the original V_β , the zero-point energy of the octupole vibrations, which turns out to depend on the value of β . We must observe, however, that the “model potential” which determines the properties of the motion in the β degree of freedom certainly include the zero-point energies of all ignored degrees of freedom of the system, first-of-all those related to the single-nucleon ones, which certainly depend on the deformation parameters. The evolution of this effective potential determines the pattern of the phase transition, and in particular the position of the critical point.

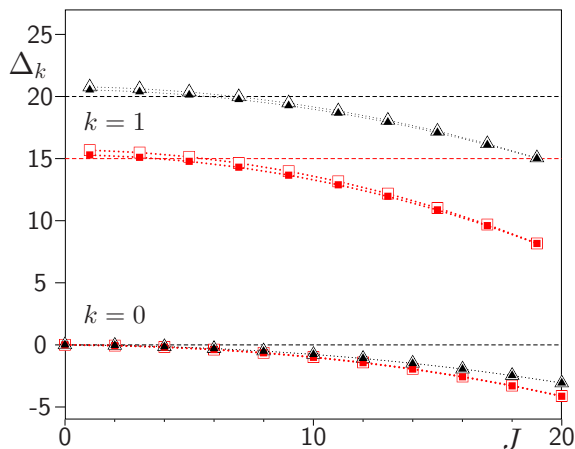


FIG. 3: (color on line) Values of $\Delta_k(J) = A'_k(J) - A'_0(0)$, as a function of J , with different assumptions on the potential-like term U_δ (or \tilde{U}_δ). The index $k=0$ corresponds to even parity and J , $k=1$ to odd parity and J . Open symbols: $U_\delta = 0$ for $-\delta_w < \delta < \delta_w$ and $= +\infty$ outside, with $\delta_w = 0.73$ (squares, for ^{150}Nd) or $\delta_w = 0.62$ (triangles, for ^{152}Sm). Full symbols: for $\tilde{U}_\delta = 0$ (instead of $U_\delta = 0$), and $\delta_w = 0.695$ or $\delta_w = 0.60$, respectively. The horizontal dashed lines correspond to the constant values used to approximate $\Delta_k(J)$ for ^{152}Sm and ^{150}Nd ($\Delta_1 = 20$ and $\Delta_1 = 15$, respectively).

It remains now to solve the β dependent equation (second line of Eqs. 12) with $\tilde{V}_\beta = 0$ and with the boundary conditions $\psi(0) = \psi(\beta_w) = 0$. Neglecting the J dependence of Δ_k , and with the new substitutions $\beta = z/\sqrt{\epsilon_k}$, $\psi(\beta) = \sqrt{z} \xi_\nu(z)$, we can transform this equation into the classical Bessel equation of order $\nu = \nu_k \equiv \sqrt{A_J + 9/4 + \Delta_k}$:

$$\frac{d^2}{dz^2} \xi_\nu(z) + \frac{1}{z} \frac{d}{dz} \xi_\nu(z) + \left[1 - \frac{\nu^2}{z^2} \right] \xi_\nu(z) = 0 \quad (13)$$

The boundary condition at the upper border is satisfied if $z_s(\nu) \equiv \beta_w \sqrt{\epsilon_s}$ is the s^{th} zero of the Bessel function $J_\nu(z)$, and therefore the eigenvalues of ϵ are given by

$$\epsilon_{k,s} = [z_s(\nu_k)/\beta_w]^2 \quad (14)$$

For $k=0$ (even parity and J), $\Delta_0 = 0$ and we obtain again, as expected, the X(5) level scheme. For $k=1$, we obtain the level sequence of the odd parity, odd- J part of the band. The comparison with experimental level schemes of ^{152}Sm and ^{150}Nd (Fig 2) shows that a satisfactory agreement can be obtained assuming a constant Δ_1 equal to 20 for ^{152}Sm and to 15 for ^{150}Nd .

To check the effect of the J dependent term in the first of Eqs. 12, it is necessary to assume a definite form for the potential U_δ (or, if we prefer, for \tilde{U}_δ). As both A'_1 and A'_0 become a function of J , we must be prepared to find some differences between the level scheme resulting from the present model and the one of X(5), also for the

ground-state band. It is matter to see how large these differences are.

In Fig. 3, the dependence of Δ_k on the angular momentum is depicted for situations close to the experimental ones of ^{152}Sm and ^{150}Nd . In Fig. 4, the differences between the experimental level energies (in units of $E(2^+)$) and those deduced with these J -dependent values of Δ_k or corresponding to constant Δ_k are also reported. The differences between the different calculated values are remarkably small, and usually smaller than their deviations from the experimental ones. This result is not surprising: in fact, at small values of J the differences between the values of Δ_k resulting from the different assumptions are quite small, while at large values of J they result to be almost insignificant, in comparison to the large values of A_J . The difference between the different calculated values in the $s=2$ sector (not shown in the figure) are also very small (< 0.1 for positive parity states and < 0.7 for negative parity ones).

In most cases, the experimental values are satisfactorily reproduced. The larger deviations observed in ^{152}Sm are limited to the even J^π values (X(5) states) above 8^+ , while – surprisingly enough – the agreement is much better for the odd J values.

It remains to verify whether the average value of β_3^2 are really small enough in comparison to the average β^2 , for the values of Δ_1 which reproduce the experimental data. Actually, for a square-well potential giving $\Delta_1 = 20$ (15), the value of $\langle \sin^2 \delta \rangle$ is about 0.05 (0.09) for the positive parity part and 0.10 (0.14) for the negative-parity part of the $K=0$ band.

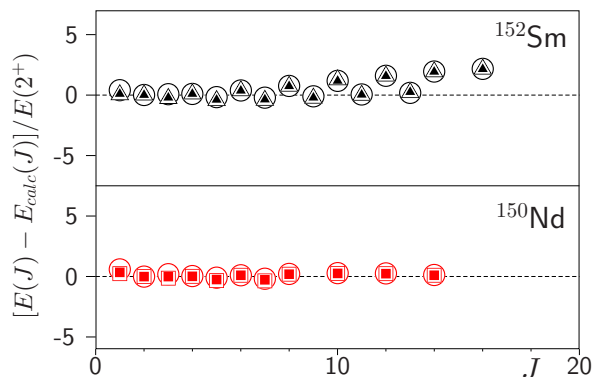


FIG. 4: (color online) Differences between the experimental energy of levels in the $K=0^\pm$ bands of ^{150}Nd and ^{152}Sm and the calculated values obtained with different assumptions, divided by the energy of the first excited state. Open circles correspond to the assumption of constant Δ_k : $\Delta_0 = 0$, *i.e.* X(5) model, for even parity and J and $\Delta_1 = 15$ (or = 20) for odd parity and J in ^{150}Nd (or ^{152}Sm). Other symbols have the same meaning as in Fig. 3.

TABLE I: Measured values [21, 22] of B(E1) in ^{152}Sm , compared with calculated ones for constant $\Delta_1 = 20$, normalized to the $1^- \rightarrow 0^+$ transition.

Transition $s_i, J_i^\pi \rightarrow s_f, J_f^\pi$	E_i [keV]	E_γ [keV]	B(E1) [10^{-3} W.u.]	
			Experimental	Calculated
$1, 1^- \rightarrow 1, 0^+$	963	963	4.2 (4)	4.2 (norm.)
$1, 1^- \rightarrow 1, 2^+$	963	841	7.7 (7)	9.8
$1, 3^- \rightarrow 1, 2^+$	1041	919	8.0 (16)	6.3
$1, 3^- \rightarrow 1, 4^+$	1041	675	8.4 (4)	10.0
$1, 5^- \rightarrow 1, 4^+$	1222	855	4.1 (9)	8.0
$1, 5^- \rightarrow 1, 6^+$	1222	675	5.0 (12)	11.1
$2, 1^- \rightarrow 2, 0^+$	1681	996	2.1 (2)	1.93
$2, 1^- \rightarrow 2, 2^+$	1681	870	5.4 (5)	5.21
$2, 3^- \rightarrow 2, 2^+$	1779	969	2.4 (5)	3.14
$2, 3^- \rightarrow 2, 4^+$	1779	756	3.9 (8)	5.91
$1, 1^- \rightarrow 2, 0^+$	963	279	(weak)	2.70
$1, 1^- \rightarrow 2, 2^+$	963	153	0.13 (4)	4.47
$2, 1^- \rightarrow 1, 0^+$	1681	1681	0.041 (6)	0.001
$2, 1^- \rightarrow 1, 2^+$	1681	1559	0.076 (9)	0.021
$2, 3^- \rightarrow 1, 2^+$	1779	1657	0.019 (4)	0.001
$2, 3^- \rightarrow 1, 4^+$	1779	1413	0.019 (4)	0.109

IV. THE TRANSITION AMPLITUDES

In the frame of the X(5) model, the E2 transition operator is defined as $\mathcal{M}(E2) \propto \beta^2 Y^{(2)}$, and its matrix elements can be easily evaluated by means of standard tensor algebra [2], as well for the negative parity as for the positive parity sector. Unfortunately, in-band E2 transitions between negative parity states cannot compete with the predominant E1 decay. Three inter-band transitions between equal-parity states have been reported [21] but two of them can be mixed M1-E2, with unknown mixing ratios. Therefore, in order to check the validity of the present extension of the X(5) model, it is necessary to investigate the E1 transitions.

In the limit of the original Bohr model (*i.e.*, assuming a constant charge density of the nuclear matter) all E1 transitions are strictly forbidden. If one assumes that the nuclear matter possesses, to some extent, an *electric polarizability*, the E1 operator takes the form [23, 24] $\mathcal{M}(E1) \propto \beta_2 \beta_3 Y^{(1)}$ that we actually used in our previous works [1, 2]. Relative values of the E1 transition amplitudes have been evaluated in the frame of the present model, using the wavefunctions corresponding to the value $\Delta_1 = 20$ appropriate for ^{152}Sm . In Table I, calculated values of B(E1) are compared with available experimental data [21, 22].

TABLE II: Measured [4, 21] and calculated values of B(E2) in ^{152}Sm , normalized to the $2^+ \rightarrow 0^+$ transition. New results, concerning the negative parity sector [21], are shown in bold.

Transition $s_i, J_i^\pi \rightarrow s_f, J_f^\pi$	E_i [keV]	E_γ [keV]	B(E2) [W.u.]	
			Experimental	Calculated
$1, 2^+ \rightarrow 1, 0^+$	122	122	144 (4)	144 (norm.)
$1, 4^+ \rightarrow 1, 2^+$	366	244	209 (7)	230
$1, 6^+ \rightarrow 1, 4^+$	707	341	245 (16)	285
$1, 8^+ \rightarrow 1, 6^+$	1125	418	285 (4)	328
$1, 10^+ \rightarrow 1, 8^+$	1609	484	320 (9)	361
$2, 2^+ \rightarrow 2, 0^+$	810	125	111 (2)	114
$2, 4^+ \rightarrow 2, 2^+$	1023	213	204 (5)	173
$2, 0^+ \rightarrow 1, 2^+$	685	573	33 (6)	83
$2, 2^+ \rightarrow 1, 0^+$	810	810	1 (9)	3
$2, 2^+ \rightarrow 1, 2^+$	810	688	3 (4)	11
$2, 2^+ \rightarrow 1, 4^+$	810	444	19 (4)	49
$2, 4^+ \rightarrow 1, 2^+$	1023	901	1 (4)	1
$2, 4^+ \rightarrow 1, 4^+$	1023	657	5 (4)	8
$2, 4^+ \rightarrow 1, 6^+$	1023	316	4 (4)	37
$2, 1^- \rightarrow 1, 3^-$	1681	640	8.4 (17)	19
$2, 1^- \rightarrow 1, 1^-$	1681	268	≤ 11 (2)	10
$2, 3^- \rightarrow 1, 3^-$	1779	738	≤ 46 (9)	6

V. COMPARISON WITH EXPERIMENTAL DATA

In Fig. 2, the calculated level energies are compared with the experimental ones for ^{150}Nd and ^{152}Sm . As for the positive parity states, our results obviously coincide with the standard X(5) model². The negative parity states are evaluated in the present model, using only one additional parameter (Δ_1). For the $s = 1$ negative parity band, the observed agreement (Fig. 4) is comparable with (and perhaps better than) the one reported for the positive parity states. In both cases, however, the first 1^- level results to be somewhat lower than the experimental one.

As for the $s = 2$ part of the spectrum, it is well known that the position of the 0_2^+ predicted by the X(5) model [3] is in satisfactory agreement with the experimental one, but the energy spacings between positive parity levels are appreciably larger than the experimental values. In ^{152}Sm , we have some information also on the negative parity states of the $s = 2$ sector. The tentative identification [14] of the 1^- state at 1681 keV as the lowest state of the negative parity part of this band has been confirmed by the recent measurements by Gar-

² A few small deviations from the published values are presumably due to different rounding errors.

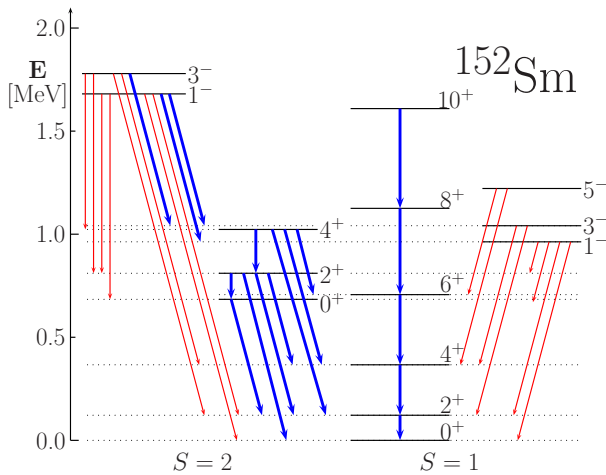


FIG. 5: (color on line) Experimentally observed transitions in $K = 0$ bands of ^{152}Sm , whose strengths are reported in [4, 21, 22]. Thinner lines: E1 transitions; thicker ones: E2 or E2/M1. Intra-band transitions are shown as vertical lines, inter-band ones as inclined lines.

rett *et al.* [21], who also identified the next level, with $J^\pi = 3^-$, at 1779 keV. Both levels are much lower than those calculated in the present model: we can conclude that this is a systematic effect for all $s = 2$ levels predicted in the frame of the X(5) model, apart from the 0^+ band head.

A more sensitive test of the model, concerning the E1 electromagnetic transitions, is only possible for ^{152}Sm (see Fig. 5). In Table I, the experimental values of E1 reduced strengths are compared with the calculated ones. Since the value of Δ_1 used in the present calculation has been fixed by level energies, no additional free parameters are used, apart from a common factor of scale which has been normalized to the $B(\text{E1}, 1^- \rightarrow 0^+)$. For the in-band transitions, the agreement is satisfactory up to the 3^- state of both the $s = 1$ and $s = 2$ bands. Experimental $B(\text{E1})$ values for transitions from the $s = 1, 5^-$ state result to be appreciably smaller than expected. A large disagreement is found for the two inter-band transitions from the $s = 1, 1^-$ to the $s = 2, 0^+$ and 2^+ levels, for which our model predicts a relatively large value of $B(\text{E1})$, at variance with experimental results reported in the NNDC tabulation [22]. For the $s = 2 \rightarrow s = 1$ inter-band transitions, the model predicts very small values of $B(\text{E1})$. Experimental values are also very small, but not in agreement with the calculated ones. One has, however, to remember that also in the positive parity sector, a significant disagreement is found between X(5) predictions and experimental $B(\text{E2})$ values for inter-band transitions.

For comparison, X(5) predictions and available experimental values for reduced E2 strengths in the positive parity sector are reported in Table II. Finally, in the

last three rows of Table II, one known value and two upper limits for the reduced E2 strengths from $s = 2$ to the $s = 1$ negative parity levels, deduced from the new experimental results of [21] are compared with the calculated values. The experimental $B(\text{E2})$ for the $s = 2, 1^- \rightarrow s = 1, 3^-$ transition results to be less than one half of the calculated one. For the $s = 2, 1^- \rightarrow s = 1, 1^-$ and $s = 2, 3^- \rightarrow s = 1, 3^-$ transitions, only upper limits of $B(\text{E2})$ are known, due to the possible mixing of M1 multipolarity. These limits are consistent with the calculated values.

VI. DISCUSSION

We can conclude that the present model is able to satisfactorily account for the lowest octupole excitations of ^{150}Nd and ^{152}Sm . From the comparison of level energies, also in the negative-parity sector, both ^{150}Nd and ^{152}Sm (and, perhaps, more ^{150}Nd than ^{152}Sm) result to be very close to the critical-point behavior, as it is defined by X(5) and by the present model.

As for the electromagnetic transition strengths, sufficient data on E1 transitions are only available for ^{152}Sm . The comparison of these data with our model predictions shows a comparable degree of success and comparable limitations as for the E2 transitions in the original X(5) model. In fact, for both nuclei, the E2 strengths are in satisfactory agreement with X(5) predictions in the case of lower lying intra-band transitions, while for inter-band transitions the calculated values are usually larger than experimental ones [4, 5]. This fact shows that the overlap between $s = 1$ and $s = 2$ wavefunctions resulting from the square-well potential is too large. Perhaps a slightly different potential well as, *e.g.*, the one discussed by Caprio [25], could improve the agreement with experimental data, also for what concern the level spacing in the $s = 2$ band, but at the expenses of having one more parameter in the model. The failure of the model to reproduce the high-spin levels, and the electromagnetic transitions between them, can be ascribed to several possible reasons. First, we must note that other levels with the same J^π as the ones of the $s = 1$ or $s = 2$ bands appear above an excitation energy of about 1.2 MeV. Part of them also have collective character, as those of the $K^\pi = 1^-$ band based on the 1511 keV level of ^{152}Sm (see Fig. 2), and probably mix, to some extent, with those considered here, due to Coriolis interactions. Moreover, the internal structure of the rotating and oscillating nucleus can be altered by the effect of Coriolis forces in their non-inertial reference frame, and the shape of the effective potential in the collective coordinates could change accordingly [26–28].

We must remind that a model like X(5) (and its present extension to the axial octupole mode) is not intended to be able of reproducing the properties of an entire class of nuclei, but is more like a bench-mark [29] saying how close a given nucleus is to the critical point of the shape

phase transition. It would not be surprising, therefore, if a similar degree of agreement can be obtained in the frame of a more general model involving a much larger number of adjustable parameters, such as the *spdf*-IBM [21, 30] or the coherent-coupling model by Minkov *et al.* [31].

Within its obvious limits, however, the proposed model seems to be able to reproduce (with only one more parameter) the $K^\pi = 0^-$ octupole bands of ^{150}Nd and ^{152}Sm and at least the in-band E1 transitions in ^{152}Sm with a comparable degree of accuracy as the original X(5) model does for the positive-parity ones.

-
- [1] P.G. Bizzeti and A.M. Bizzeti-Sona, Phys. Rev. C **70**, 064319 (2004).
- [2] P.G. Bizzeti and A.M. Bizzeti-Sona, Phys. Rev. C **77**, 024320 (2008).
- [3] F. Iachello, Phys. Rev. Lett. **87**, 052502 (2001).
- [4] R.F. Casten and N.V. Zamfir, Phys. Rev. Lett. **87**, 052503 (2001).
- [5] R. Krucken *et al.*, Phys. Rev. Lett. **88**, 232501 (2002).
- [6] R. Clark *et al.*, Phys. Rev. C **68**, 037301 (2003).
- [7] Z.P. Li, T. Niksic, D. Vretenar, J. Meng, G.A. Lalazissis, and P. Ring, Phys. Rev. C **79**, 054301 (2009).
- [8] L.M. Robledo, R.R. Rodriguez-Guzman, and P. Sarriguren, Phys. Rev. C **78**, 034314 (2008).
- [9] J. Meng, W. Zhang, S. Zhou, H. Toki, and L. Geng, Eur. Phys. J. A **25**, 23 (2005).
- [10] D. Tonev, A. Dewald, T. Klug, P. Petkov, J. Jolie, A. Fitzler, O. Moller, S. Heinze, P. von Brentano, and R.F. Casten, Phys. Rev. C **69**, 034334 (2004).
- [11] O. Moller *et al.*, Phys. Rev. C **74**, 024313 (2006).
- [12] P.G. Bizzeti and A.M. Bizzeti-Sona, Phys. Rev. C **66**, 031301(R) (2002).
- [13] P.G. Bizzeti and A.M. Bizzeti-Sona, in *Nuclear Theory 24*, edited by S. Dimitrova (Heron Press, Sofia, 2005), p. 311.
- [14] P.G. Bizzeti and A.M. Bizzeti-Sona, in *Collective motion and Phase transitions in Nuclear Systems*, edited by A. Raduta, V. Baran, A. Gheorghe, and I. Ursu (World Scientific, 2006), p. 3.
- [15] D.A. Bohr, Dan. Mat. Phys. Medd. **26** (1952).
- [16] A. Raduta, C. Raduta, and A. Faessler, Phys. Lett. B **635**, 80 (2006).
- [17] A. Raduta and C. Raduta, Nuclear Phys. **A768**, 170 (2006).
- [18] J. Eisenberg and W. Greiner, *Nuclear Theory*, vol. I (Amsterdam, 1987), 3rd ed.
- [19] W. Pauli, in *Handbook der Physik*, edited by A. Smekal (Springer, Berlin, 1933), vol. V/I.
- [20] D. Bonatsos, D. Lenis, N. Minkov, D. Petrellis, and P. Yotov, Phys. Rev. C **71**, 064309 (2005).
- [21] P. Garrett *et al.*, Phys. Rev. Letters **103**, 062501 (2009).
- [22] <http://www.nmdc.bnl.gov/>.
- [23] D. A. Bohr and B. Mottelson, Nuclear Phys. **4**, 529 (1957).
- [24] D. A. Bohr and B. Mottelson, Nuclear Phys. **9**, 687 (1958).
- [25] M.A. Caprio, Phys. Rev. C **69**, 044307 (2004).
- [26] E. Williams, R.J. Casperson, and V. Werner, Phys. Rev. C **77**, 061302(R) (2008).
- [27] P. Cejnar, Phys. Rev. Lett. **90**, 112501 (2003).
- [28] P. Cejnar, Phys. Rev. C **65**, 044312 (2002).
- [29] R.F. Casten, N.V. Zamfir, and R. Krucken, Phys. Rev. C **68**, 059801 (2003).
- [30] M. Babilon, N.V. Zamfir, D. Kusnezov, E.A. McCutchan, and A. Zilges, Phys. Rev. C **72**, 064302 (2005).
- [31] N. Minkov, P. Yotov, S. Drenska, W. Scheid, D. Bonatsos, D. Lenis, and D. Petrellis, Phys. Rev. C **73**, 044315 (2006).